A systematic analysis of the spectra of the lanthanides doped into single crystal LaF_3 [a]

W. T. Carnall, G. L. Goodman, K. Rajnak,[b] and R. S. Rana[c]
Chemistry Division, Argonne National Laboratory, Argonne, Illinois 60439

(Received 27 October 1988; accepted 21 December 1988)

The optical spectra of the lanthanides doped into single crystal LaF_3 have been interpreted in terms of transitions within $4f^N$ configurations. Energy matrices combining free-ion terms with a crystal field for an approximate model which assumes C_{2v} instead of the actual C_2 site symmetry were diagonalized. Excellent correlations were obtained between experimental transition energies and the computed level structures. We also report the results of previously unpublished experimental spectroscopic investigations of Nd^{3+} and Sm^{3+}:LaF_3, as well as predicted energy levels for Pm^{3+}:LaF_3. The spectroscopic data for each ion were independently interpreted using an effective-operator model, then the model parameters were intercompared. Systematic trends have been identified, and a comprehensive energy level diagram is presented.

INTRODUCTION

The low-temperature absorption and luminescence spectra of trivalent lanthanide ions, Ln^{3+}, doped into single crystal LaF_3, Ln^{3+}:LaF_3, in the range 0–50 000 cm^{-1} exhibit a narrow band structure characteristic of transitions between states within the $4f^N$ configuration. These transitions are interpreted as connecting the ground state to upper-state energy levels, and their energies are used to define the parameters of an effective Hamiltonian which reproduces the complete structure of the crystal-field split $4f^N$ configuration.

Parameters associated with the effective interactions derived independently from the spectrum of each individual lanthanide ion show a systematic variation across the lanthanide series. As expected, the free-ion interactions in LaF_3 are depressed somewhat relative to those derived from atomic spectra, and this may be taken as evidence for ligand contributions to optically active orbitals. However, the highly ionic character of the LaF_3 lattice appears to make the fitted parameters a rather good approximation to true free-ion interactions, and a useful basis for comparison with spectra in other crystalline environments as well as with *ab initio* calculations.

Tabulations of energy levels of lanthanides doped into various crystal lattices,[1,2] as well as expositions of the basic theory of atomic and crystal-field interactions in f^N configurations, are to be found in the literature.[3–7] However, much of the extensive spectroscopic data for Ln^{3+}:LaF_3 were published before crystal-field calculations for low site symmetries were common. Typically, an average energy or center of gravity over a group of levels apparently belonging to a particular J state was taken as the free-ion energy of the state. Crystal-host-dependent "free-ion" parameters were then derived via a process of least-squares fitting.

The site symmetry of La^{3+} in LaF_3 is C_2,[8] but it can be approximated either as C_{2v} or as D_{3h}. This fact apparently led to some confusion in early crystallographic work, and it also influenced the initial crystal-field analyses. Onopko[9] was the first to publish crystal-field parameters for Nd^{3+}:LaF_3 and Er^{3+}:LaF_3 in D_{3h} symmetry which we found could yield calculated sets of energy levels for each free-ion J state in those ions consistent with the observed splitting pattern of the state. Parameter fitting based on Onopko's results also provided the basis for classification of a considerable amount of data for other Ln^{3+} with odd N.[10,11] For all f^N configurations with odd N the maximum number of crystal-field components in a state with quantum number J is $J + 1/2$ in any symmetry lower than cubic. However, when N is even, a lower symmetry than D_{3h} must be used to completely remove the symmetry-related degeneracy of each state. Morrison and Leavitt[12] reported parametrized crystal-field calculations in the actual C_2 symmetry based on a limited number of states in each $4f^N$ configuration in LaF_3. They did not examine in detail the behavior of the free-ion operators, nor did they atempt to reanalyze the data.

In the present investigation, we have used a C_{2v} crystal field and have performed simultaneous diagonalizations of the free-ion and crystal-field interactions. We have reevaluated the original assignments in our own published work as well as that of others. We also present additional new data to complete the series. While a C_{2v} symmetry removes all the symmetry-imposed degeneracy in even N systems, a primary reason for the approximation is that it is more tractable than C_2 symmetry for computational purposes. Thus our intent

[a] Work performed under the auspices of the Office of Basic Energy Sciences, Division of Chemical Sciences, U. S. Department of Energy, under Contract No. W-31-109-ENG-38.

[b] Current address: Physics Department, Kalamazoo College, Kalamazoo, MI 49007.

[c] Current address: Physics Department, College of the Holy Cross, Worcester, MA 01610.

was to use a sufficiently detailed theoretical model to interpret a large body of experimental data, to highlight systematic trends, and to provide a basis for prediction of the energies of transitions not observed or beyond the normal optical range.

We began with modeling the extensive spectra of Nd^{3+}:LaF_3 and Er^{3+}:LaF_3 in D_{3h} site symmetry.[11] The fitting process was then repeated in the C_{2v} approximation. While, as expected, the overall agreement between theory and experiment did not improve, the magnitude of each of the crystal-field parameters in the C_{2v} set was statistically determined even though there are nine crystal-field parameters for C_{2v} and only four for D_{3h}. We proceeded by using the C_{2v} parameter sets for Nd^{3+} and Er^{3+}:LaF_3 as models for interpretating the spectra of adjacent ions with even numbers of f electrons. Since crystal-field parameters in Ln^{3+}:$LaCl_3$ exhibit only moderate variation over the series,[2,10] the parameters for one ion serve as a reasonable approximation of those for nearest neighbor ions. Thus, we used the crystal-field deduced for Er^{+}:LaF_3 as a reasonable starting approximation for both Ho^{3+}:LaF_3 and Tm^{3+}:LaF_3, combining it with free-ion parameters characteristic of Ho^{3+} and Tm^{3+}, respectively. Use of the above principle has now led to consistent analyses of experimental $f\rightarrow f$ spectra for all Ln^{3+}:LaF_3 except Pm^{3+}:LaF_3. Progress reports in this investigation are given in Refs. 13–16. Polarization and Zeeman-effect data provided an independent means of assigning crystal-field states in Ln^{3+}:$LaCl_3$ spectra,[1] but in LaF_3 attempts to interpret polarization measurements have met with limited success.[6,7] This lack of an independent check on assignments is a disadvantage since there is no assurance that all of the correlations based on energy are correct.

EXPERIMENTAL

Extensive spectra for most lanthanides doped into LaF_3 including both published and unpublished work from this laboratory were reanalyzed. Since the crystals were obtained from a commercial source,[17] the radioactivity associated with Pm unfortunately excluded it from study. Moreover, limited data are available for the Eu^{3+} system.[7,18] Measurements in most of the Ln^{3+}:LaF_3 systems were made using several different (0.1%–2%) concentrations of the lanthanide impurity in LaF_3. Spectra in the range ~4000–15 000 cm^{-1} were recorded using a Cary model 14R (crystal-grating 0.5 m monochromator) recording spectrophotometer. In the region 15 000–50 000 cm^{-1}, both a 1 m Hilger–Engis model 1000 spectrograph equipped with an EMI 9558 Q photomultiplier, and the Argonne 30 ft Paschen–Runge spectrograph (in second order) were used. Spectra were usually recorded at ~298, 77, and 4 K.

Early conflicting x-ray structure reports suggesting C_{2v}[19] or D_{3h}[20] site symmetries were resolved with subsequent studies[8,21,22] showing that the nine nearest-neighbor F^- ions present a sufficiently distorted environment so that the symmetry is $D^4_{3d}(P\bar{3}c1)$ with a C_2 point symmetry at the La site. A powder neutron-diffraction study of LaF_3 and CeF_3 provided additional confirmation of the latter structure.[23] Isostructural members of the series are LaF_3, CeF_3, PrF_3, and NdF_3; SmF_3 and the heavier trifluorides are dimorphic and also crystallize in the orthorhombic YF_3 lattice.[24]

THEORETICAL TREATMENT OF EXPERIMENTAL DATA

Developing a complete Hamiltonian for $4f^N$ configuration relies on two important physical assumptions: first, we assume that these electronic states are well removed from other electronic states of the complex; and second, that the influence of the nonspherically symmetric part of the electric field due to the solid state environment of the rare earth ion can be treated as a small perturbation of the f^N free-ion configuration. Thus, we approach the calculation of these electronic properties in two stages. The first deals with the energy-level structure of the gaseous free-ion, and the second with the additional (crystal-field) interactions which arise when the ion is in a condensed phase. The free-ion Hamiltonian is assumed to be the same in both cases.

The interactions primarily responsible for the free-ion structure in trivalent lanthanides are the electrostatic repulsion between electrons in the f^N configuration and the coupling of their spin and orbital angular momenta. Since the treatment of these primary and other smaller but essential contributions to the effective operator Hamiltonian of the system has been covered in a recent extensive review,[25] we limit the present discussion to an identification of the parameters and the corresponding operators of the parametric model. The Hamiltonian is written

$$H = H_0 + \sum_{k=0,2,4,6} F^k(nf,nf) f_k + \zeta_f A_{SO} + \alpha L(L+1) + \beta G(G_2) + \gamma G(R_7) + \sum_{i=2,3,4,6,7,8} t_i T^i + \sum_{h=0,2,4} m_h M^h + \sum_{f=2,4,6} p_f P^f + \sum_{k,q,i} B^{(k)}_q C^{(k)}_q(i) .$$

Here H_0 is the spherically symmetric one-electron part of the Hamiltonian. The F^k and ζ_f are the electrostatic and spin–orbit integrals; f_k and A_{SO} represent the angular parts of the electrostatic and spin–orbit interactions, respectively. The parameters associated with the two-body correction terms are designated α, β, and γ; $G(G_2)$ and $G(R_7)$ are Casimir's operators for the groups G_2 and R_7, and L is the total orbital angular momentum.[26]

For configurations of three or more equivalent f electrons, three-particle configuration interaction terms are included in the form given by Judd.[27,28] Such terms arise from the perturbing effects of those configurations that differ from f^N in the quantum numbers of a single electron. They are expressed as $t_i T^i$ ($i = 2, 3, 4, 6, 7, 8$), where T^i are the parameters and t_i are three-particle operators. Four-particle and higher order terms could be defined for appropriate configurations. However, they do not appear to be necessary to a good representation of the experimental data.

Magnetically correlated corrections were also introduced using the form suggested by Judd *et al.*[29] Values of the

Marvin integrals,[30] M^h ($h = 0, 2, 4$), which represent spin–spin and spin–other–orbit relativistic corrections, have been determined from parametric fits to some experimental data, and were found to be similar to those computed using *ab initio* methods. Of the two-body magnetic corrections, the most important appears to be the electrostatically correlated spin–orbit perturbation which involves the excitation of an f electron into a higher-lying f shell. The corresponding parameters are P^f ($f = 2, 4, 6$). The operators associated with the magnetically correlated corrections are designated m_h and p_f, respectively.

Although extensive corrections to the basic free-ion Hamiltonian have been developed, crystal-field calculations are usually carried out using a single-particle crystal-field theory[4,5] in which the parameters are appropriate to a given site symmetry:

$$H_{\mathrm{CF}} = \sum_{k,q,i} B_q^{(k)} C_q^{(k)}(i) , \tag{6}$$

where $C_q^{(k)}(i)$ is a spherical tensor of rank k depending on the coordinates of the ith electron and the summation involving i is over all f electrons of the ion of interest; the values of k and q for which the parameters $B_q^{(k)}$ are nonzero depend on the site symmetry. For configurations (f^4–f^{10}) in which the Hamiltonian matrices including the C_{2v} crystal field are greater than 200 by 200, we have used a method of truncation to select manageable portions of this matrix. The eigenstates of the free-ion Hamiltonian provide the basis states for these truncations.[25]

ANALYSIS OF EXPERIMENTAL DATA

The procedure we used to fit spectra of Ln^{3+}:LaF_3 yields a local rather than global minimum for the fitting function. The whole range of parameter values can therefore be viewed as made up of several domains within each of which a converged set of fitting parameters can be found. But the transition from one of these domains to another would require the sum of squared residuals to become so large that it does not occur in our search. The D_{3h} and the C_{2v} models for the crystal environment of the La site in LaF_3 fall into two such distinct domains. Thus, when at first we started from a reasonable fit to odd electron systems based on the D_{3h} model and then added the extra five parameters required for a C_{2v} model, we found it quite difficult to determine values for these extra parameters. In some cases even the signs of some parameters were indeterminate. This approach has also been discussed by Caro and co-workers.[31] In our second approach we started with initial values for the parameters B_q^k equal to the real parameters calculated by Morrison and Leavitt[12] using the method of lattice sums for the C_2-axis setting in LaF_3. In this second parameter domain the C_{2v} model appears to be well behaved, yielding well-determined values for most of the C_{2v} crystal-field parameters for the lanthanides in LaF_3, as reported below.

SUMMARY OF EXPERIMENTAL DATA

The following summary of experimental results for Ln^{3+}:LaF_3 does not attempt to be a review of the literature. References are limited to more extensive experimental investigations. The bulk of the tabulated experimental data taken in absorption was drawn from measurements made in the course of the present investigation. The fluorescence and far-infrared spectra are quoted from the literature. All data are reported in cm^{-1} (vacuum).

Nd^{3+}:LaF_3($4f^3$)

The absorption spectrum of Nd^{3+}:LaF_3 played a critical role in the analysis of other light lanthanide spectra. The crystal-field parameters determined for Nd^{3+}:LaF_3 were used to model the energy level structures for Pr^{3+} and Pm^{3+}, as well as Sm^{3+}:LaF_3.

There are extensive published reports of the structure observed in low-temperature absorption and fluorescence spectra of Nd^{3+}:LaF_3.[6,32–34] These data have been augmented and extended beyond $\sim$24 000 cm^{-1} by previously unpublished work at ANL[11] to provide a relatively complete set of crystal-field components. Of the 182 levels in the f^3 configuration, 146 were assigned, Appendix I.[35] Only one $^2F_{7/2}$ and one $^2F_{5/2}$ state lie beyond the present range of observation. Thus both the atomic and crystal-field parameters, Table I, are considered well determined. The possible exception is γ whose value is partially determined by available data but is strongly dependent on the position of the missing ^2F levels.

Pr^{3+}:LaF_3($4f^2$)

Spectroscopic investigations at several different laboratories using moderate to high resolution have identified crystal-field components of most of the states of Pr^{3+}:LaF_3.[36–42] One of the weak points in the theoretical analysis has been the lack of rationale for unique assignments to components of the $^1I_6$ state. It has not been possible to distinguish apparent vibronic structure, possibly in part associated with $^3P_1$ levels, from expected very low intensity electronic transitions to the $^1I_6$ state. As it turns out, the two-body operator parametrized by α is essentially defined by the energy of the $^1I_6$ state. Changes in α can shift the center of gravity of $^1I_6$ with respect to that of $^3P_1$ with little if any affect on the computed level energies for the rest of the configuration.

The model crystal field for Pr^{3+}:LaF_3 based on parameters for Nd^{3+}:LaF_3, with an earlier approximate set of free-ion parameters,[36] yielded an energy level scheme that was generally in very good agreement with the experimental data.[13] As anticipated, several modifications of the original assignments were indicated. Apparent correlation between predicted and observed structure in the range of the $^1I_6$ state could be made, but there was no basis for unique assignment.

The recent measurements of the energy of the $^1S_0$ level[41,42] are more accurate than, but within the limits of error of, our previous value.[36] If we take the new value together with the reported energies of transitions from $^1S_0$ to levels of the $^3F_4$, $^1G_4$, and $^1I_6$ states[40] and correct to cm^{-1} vac, several new assignments can be made, Table II.

In the $^3F_4$ state, the 7025 cm^{-1} fluorescence line from $^1S_0$ agees well with a transition observed in absorption,[13] as does that at 7105 cm^{-1}, whereas the 7089 cm^{-1} line must according to the model calculation, refer to another, possibly a perturbed site. We do see evidence of sideband structure at

TABLE I. Energy level parameters for Ln^{3+}:LaF_3 (in cm^{-1}).[a]

	Ce	Pr	Nd	Pm	Sm	Eu	Gd	Tb	Dy	Ho	Er	Tm	Yb
F^2		68 878(23)	73 018(19)	76 400	79 805(16)	83 125(31)	85 669(17)	88 995(58)	91 903(69)	94 564(38)	97 483(32)	100 134(23)	
F^4		50 347(69)	52 789(94)	54 900	57 175(45)	[59 268 *R*]	[60 825 *R*]	[62 919 *R*]	64 372(147)	66 397(64)	67 904(67)	69 613(62)	
F^6		32 901(37)	35 757(42)	37 700	40 250(26)	[42 560 *R*]	44 776(24)	47 252(72)	49 386(139)	52 022(63)	54 010(60)	55 975(104)	
ζ	647.3(11)	751.7(2)	885.3(1)	1 025	1 176(1)	1 338(3)	1 508(2)	1 707(2)	1 913(2)	2 145(1)	2 376(2)	2 636(1)	2 928(10)
α		16.23(0.23)	21.34(0.14)	20.50	20.16(0.89)	[20.16]	18.92(0.83)	18.40(0.19)	18.02(0.23)	17.15(0.11)	17.79(0.20)	17.26(0.30)	
β		− 566.6(15)	− 593.0(8)	− 560	− 566.9(8)	[− 566.9]	[− 600]	− 590.9(29)	− 633.4(10)	− 607.9(6)	− 582.1(10)	− 624.5(15)	
γ		1371(13)	1445(16)	1475	[1500]	[1500]	[1575]	[1650]	1790(47)	[1800]	[1800]	[1820]	
T^2			298(6)	300	[300]	[300]	[300]	[320]	329(9)	[400]	[400]	[400]	
T^3			35(3)	35	[36]	[40]	[42]	[40]	36(5)	37(2)	43(5)		
T^4			59(4)	58	[56]	[60]	[62]	[50]	127(22)	107(5)	73(5)		
T^6			− 285(6)	− 310	− 347(7)	[− 300]	[− 295]	− 395(28)	− 314(16)	− 264(16)	− 271(11)		
T^7			332(8)	350	373(7)	[370]	[350]	303(17)	404(8)	316(20)	308(18)		
T^8			305(10)	320	348(5)	[320]	[310]	317(13)	315(7)	336(8)	299(17)		
$M^{0,b}$		2.08(0.3)	2.11(0.1)	2.4	2.60(0.1)	[2.1]	3.22(0.2)	2.39(0.1)	3.39(0.1)	2.54(0.1)	3.86(0.2)	3.81(0.3)	
$P^{2\,c}$		− 88.6(47)	192(31)	275	357(28)	[360]	676(75)	373(53)	719(30)	605(24)	594(63)	695(46)	
B_0^2	[− 218]	− 218(16)	− 256(16)	− 245	− 224(19)	− 217(56)	[− 231]	− 231(24)	− 244(18)	[− 240]	− 238(17)	− 249(14)	[− 249]
B_0^4	[738]	738(40)	496(73)	470	452(47)	413(86)	[604]	604(49)	506(43)	560(27)	453(90)	457(29)	[457]
B_0^6	[679]	679(48)	641(54)	640	649(47)	558(92)	[280]	280(38)	367(40)	376(28)	373(83)	282(42)	[282]
B_2^2	[− 50]	− 120(13)	− 48(12)	− 50	[− 50]	[− 50]	[− 99]	− 99(16)	− 65(12)	− 107(10)	− 91(14)	− 105(9)	[− 105]
B_2^4	[431]	431(27)	521(39)	525	597(29)	[597]	[340]	340(34)	305(33)	250(19)	308(60)	320(21)	[320]
B_4^4	[616]	616(27)	563(41)	490	408(28)	[408]	[452]	452(31)	523(25)	466(19)	417(56)	428(22)	[428]
B_2^6	[− 921]	− 921(32)	− 839(39)	− 750	− 706(33)	[− 706]	[− 721]	− 721(29)	− 590(24)	− 576(18)	− 489(51)	− 482(33)	[− 482]
B_4^6	[− 348]	− 348(41)	− 408(35)	− 450	− 508(34)	[− 508]	[− 204]	− 204(29)	− 236(27)	− 227(20)	− 240(51)	− 234(36)	[− 234]
B_6^6	[− 788]	− 788(38)	− 831(41)	− 760	− 692(38)	[− 692]	[− 509]	− 509(33)	− 556(25)	− 546(22)	− 536(49)	− 492(36)	[− 492]
n^d	7	75	146		232	29	70	146	198	204	127	56	5
σ^d	51	16	14		13	16	10	12	12	10	19	10	38

[a] Values in parentheses are errors in the indicated parameters. Values in brackets were either not allowed to vary in the parameter fitting, or if followed by an *R*, were constrained: For Eu^{3+}, $F^4/F^2 = 0.713$, $F^6/F^2 = 0.512$; for Gd^{3+}, $F^4/F^2 = 0.710$; for Tb^{3+}, $F^4/F^2 = 0.707$. All parameters for Pm^{3+} are interpolated values.

[b] M^0 was varied freely, M^2 and M^4 were constrained by the ratios $M^2 = 0.56\,M^0$, $M^4 = 0.31\,M^0$.

[c] P^2 was varied freely, P^4 and P^6 were constrained by the ratios $P^4 = 0.5\,P^2$, $P^6 = 0.1\,P^2$.

[d] Deviation $(\sigma) = \Sigma[(\Delta i)^2/n - p]^{1/2}$, where Δi is the difference between observed and calculated energies, n is the number of levels fit, and p is the number of parameters freely varied.

TABLE II. Emissions from the $^1S_0$ state of Pr^{3+}:LaF_3.[a]

$S'J'$		λ(Å)	cm^{-1} (vac)	Terminal state (cm^{-1})[b]
$^1I_6$	*A*	3892	25 686	21 279
	B	3900	634	331
	C	3939	380	585
	D	3988	068	897
$^1G_4$	*A*	2686	37 219	9 746
	B	2697	067	9 898
	C	2707	36 930	10 035
	D	2716	808	057
	E	2741	472	493
$^3F_4$	*A*	2503	39 940	7 025
	B	2507	876	7 089
	C	2508	860	7 105

[a] Reference 40.
[b] Assume the initial state is in every case $^1S_0$ at 46 965 cm^{-1} (vac).[42]

this energy in absorption.

Four of the five transitions connecting $^1S_0$ to the $^1G_4$ state, reported in fluorescence, are consistent with transitions predicted by the model calculation, and with structure observed in absorption in the present experimental study.[13] There appear to be two lines, 10 035 and 10 057 cm^{-1}, which correspond to a single level observed in absorption.

The most interesting result of the reported fluorescence from $^1S_0$ is that attributed to terminal levels in the $^1I_6$ state. The model predicts a very wide splitting of $\sim$600 cm^{-1} for the $^1I_6$ state. Examining the fluorescence results, we see that they do span the predicted $\sim$600 cm^{-1}. While levels at 21 279 and 21 331 cm^{-1} do not correspond to structure observed in absorption, weak bands are observed near 21 585 and 21 897 cm^{-1}. Thus we allowed these four transitions to define the energy of the $^1I_6$ state. This, together with assignment of the $^1S_0$ state, which defines the value of γ, specifies the free-ion parameters. Only a small adjustment in the crystal field is required for an excellent correspondence between theory and experiment, Appendix II.[35] The final set of parameters values, Table I, is consistent with those originally assumed.[13] However, the interpretation remains speculative and we hope will stimulate further experimental investigations. In the last section of this paper, we note that a larger value of α than that indicated here would be more consistent with apparent systematic trends, but a larger α would shift the $^1I_6$ states to higher energies relative to $^3P_1$.

Ce^{3+}:LaF_3($4f^1$)

An examination of the infrared spectrum of Ce^{3+}:LaF_3,[43] revealed four bands that persisted at $\sim$4 K. These can be identified as the components of the $^2F_{7/2}$ multiplet. Temperature-dependent studies provided evidence for a component of the $^2F_{5/2}$ group at 150 cm^{-1}. Energy levels of the $^2F_{5/2}$ state deduced from Raman spectra were placed in the 140–170 cm^{-1} range and near 300 cm^{-1}.[44]

The crystal-field parameters obtained in the fit of data for Pr^{3+}:LaF_3 were used as a model for Ce^{3+}:LaF_3, and in the initial fitting procedure, only ζ was allowed to vary. While the resulting parameter set yielded a computed energy level scheme that was consistent with the observed structure, the correlation was significantly improved using the value $B_2^2 = -50\ cm^{-1}$ instead of $-120\ cm^{-1}$, Tables I and III.

An attempt was made to vary selected crystal-field parameters, since the whole set could not be varied simultaneously with such a limited number of observations. When B_0^4,B_0^6, and B_6^6 were varied in addition to ζ, the fit to experiment was improved but the parameter magnitudes increased relative to those for Pr^{3+}:LaF_3. Actually, an increase in the magnitude of the parameters is not unreasonable considering that the ionic radius of Ce^{3+} (1.034 Å) is considerably larger than that of the model Pr^{3+} (1.013 Å).[1] However, we confirm that the extrapolated crystal-field parameters are fully consistent with the experimental results.

Pm^{3+}:LaF_3 ($4f^4$)

The absorption spectrum of Pm^{3+}:LaF_3 has not been reported, but an extensive interpretation of the absorption and fluorescence spectra of Pm^{3+}:$LaCl_3$ has been published.[45] We have used the regularities in the energy level parameters for Ln^{3+}:LaF_3 as the basis for interpolation of approximate parameter values for Pm^{3+}:LaF_3, Table I. The corresponding computed crystal-field levels to $\sim$25 000 cm^{-1} are given in Appendix III.[35]

Sm^{3+}:LaF_3 ($4f^5$)

The observation and analysis of the absorption and fluorescence spectra of Sm^{3+}:LaF_3 in the range 0–11 000 cm^{-1} was reported by Rast, Fry, and Caspers,[46] an extended line list was given by Dieke,[1] and additional measurements to $\sim$47 000 cm^{-1} were obtained in the present investigation. A composite tabulation with most of the energy assignments based on work at ANL, is presented in Appendix IV.[35] Since the crystal-field structure of Sm^{3+} is very extensive, initial assignments were limited to the more isolated groups with the model calculation based on the crystal-field parameters for Nd^{3+}:LaF_3. With Sm^{3+}, we are only able to observe $\sim$50% of the total energy range covered by the $4f^5$ configuration. Consequently, the free-ion parameters, Table I, are

TABLE III. Experimental and computed energy level structure for Ce^{3+}:LaF_3.

SLJ state	Obs.[a] (cm^{-1})	Calc.[b] (cm^{-1})	O − C
$^2F_{5/2}$	0	−3	3
	151	152	−1
	280[c]	284	−4
$^2F_{7/2}$	2160	2235	−75
	2240	2274	−34
	2635	2586	49
	2845	2783	62

[a] Reference 43 (cm^{-1} vac).
[b] Parameter values are given in Table I.
[c] Reference 44.

not fully representative of the total configuration even though they reproduce the available data quite well. The large number of states for Sm^{3+}:LaF_3 also required truncation of the energy matrices[25] following a procedure cited in the analysis of the spectrum of Pm^{3+}:$LaCl_3$.[45] This introduces an error which is in general small, but may amount to several wave numbers for some levels.

Eu^{3+}:LaF_3 ($4f^6$)

Observation of Eu^{3+}:LaF_3 spectra in absorption and fluorescence has been reported by Kumar *et al.*[7] following earlier less extensively analyzed experiments by Weber.[18] The energy levels of the ^5D and ^7F states that can be deduced from the measurements are very similar to those reported for Eu^{3+}:$LaCl_3$.[1]

The experimental results of Kumar *et al.*[7] included polarization measurements, and the assigned energy levels in the ^7F and ^5D multiplets were identified by symmetry species assuming a C_{2v} site symmetry. The present crystal-field calculations, using the crystal-field parameters for Sm^{3+}:LaF_3 as the initial model, provide a direct comparison with these assignments. Two reported levels, Table IV, those at 2847 and 2894 cm^{-1}, were clearly inconsistent with the initial parameter set. Only a very limited refinement of the parameters could be justified based on the small number of observations; however, variation of F^2, ζ, B^2_0,B^4_0, and B^6_0, with fixed ratios of F^4/F^2 and F^6/F^2 did result in a good fit to the data and parameter values consistent with series trends, Table I. The crystal-field parameters obtained in this way were, within the errors, the same as those for Sm^{3+}:LaF_3.

The symmetry associated with the various calculated energy levels for C_{2v} symmetry can be deduced from the eigenvectors. The character table for the symmetry group, Table V, gives the characters for the twofold rotation about the z direction (C_{2z}), and the xz reflection plane (σ_{xz}), for each of the four symmetry species of the C_{2v} point group, A_1, A_2, B_1, and B_2. The conventions used here agree with those used by Kumar *et al.*[7] The eigenfunctions in the crystal-field calculation are specified in terms of basis states of well-defined total angular momentum J and its projection in the z direction, M. The effect of C_{2z} is to multiply one of these basis states by $(-1)^M$ and the effect of reflection in the xz plane is to change the state $|JM\rangle$ into the state $|J-M\rangle$ and multiply it by $(-1)^{J+M+P}$, where P is the parity of the state determined by taking the sum of the orbital angular momenta for each electron in the ion of interest. For Eu^{3+} with six f electrons, J is an integer and P is even.

Only for $M=0$ does M remain well defined for the eigenstates in C_{2v} symmetry. For other values of M, the eigenstates contain either the sum or the difference of the basis states corresponding to M and $-M$. If we use

$$|J\,|M|\,\text{plus}\rangle = [\,|J\,|M|\,\rangle + |J-|M|\,\rangle]/\sqrt{2}$$

and

$$|J\,|M|\,\text{minus}\rangle = [\,|J\,|M|\,\rangle - |J-|M|\,\rangle]/\sqrt{2}$$

for M nonzero,

the remaining three columns of Table V allow us to classify the eigenvectors for Eu^{3+} according to whether $|M|$ is even

TABLE IV. Experimental and computed energy level structure for Eu^{3+}:LaF_3.

SLJ[a] State	Obs.[b] (cm^{-1})	Species[c]	Model[d] calc. (cm^{-1})	Fit[e] calc. (cm^{-1})
$^7F_0$	0	A_1	− 10	− 13
$^7F_1$	313	A_2	318	318
	375	$B_{1(2)}$	375	372
	415	$B_{2(1)}$	414	412
$^7F_2$	964	A_1	940	943
	···	$B_{(1)}$	975	974
	997	A_1	1 011	1 012
	···	$A_{(2)}$	1 109	1 110
	1 098	B_2	1 118	1 118
$^7F_3$	···	$B_{(2)}$	1 834	1 839
	1 843	B_1	1 852	1 855
	1 867	$A_{1(2)}$	1 861	1 866
	1 884	$A_{2(1)}$	1 888	1 893
	1 889	$B_{1(2)}$	1 892	1 894
	1 908	A_2	1 923	1 919
	1 996	$B_{2(1)}$	2 007	2 010
$^7F_4$	2 614	$B_{1(2)}$	2 583	2 593
	2 788	$A_{1(2)}$	2 769	2 768
	2 852	$A_{2(1)}$	2 816	2 822
	2 873	$B_{2(1)}$	2 880	2 896
	2 926	B_2	2 890	2 900
	(2 894)	A_1	2 966	2 972
	···	$A_{(2)}$	2 988	2 987
	3 047	B_1	3 060	3 065
	3 068	$A_{2(1)}$	3 077	3 075
$^7F_5$	···	$B_{(2)}$	3 775	3 787
	···	$B_{(1)}$	3 800	3 809
	···	$A_{(1)}$	3 864	3 873
	···	$A_{(2)}$	3 921	3 931
	···	$A_{(2)}$	3 991	3 995
	···	$B_{(2)}$	3 994	4 005
	···	$B_{(2)}$	4 035	4 036
	···	$A_{(1)}$	4 050	4 056
	···	$B_{(1)}$	4 052	4 061
	···	$A_{(2)}$	4 098	4 096
	···	$B_{(1)}$	4 102	4 109
$^7F_6$	···	$A_{(1)}$	4 919	4 934
	···	$A_{(2)}$	4 935	4 950
	···	$B_{(2)}$	5 000	5 012
	···	$B_{(1)}$	5 027	5 039
	···	$A_{(1)}$	5 035	5 046
	···	$B_{(1)}$	5 036	5 046
	···	$A_{(1)}$	5 112	5 124
	···	$B_{(2)}$	5 120	5 129
	···	$A_{(2)}$	5 123	5 130
	···	$B_{(2)}$	5 140	5 151
	···	$A_{(2)}$	5 159	5 168
	···	$A_{(1)}$	5 167	5 176
	···	$B_{(1)}$	5 174	5 182
$^5D_0$	17 293	A_1	17 296	17 294
$^5D_1$	19 043	A_2	19 037	19 034
	056	B_2	055	052
	063	B_1	066	064
$^5D_2$	21 507	$B_{1(2)}$	21 512	21 512
	512	$A_{1(2)}$	525	525
	532	$B_{2(1)}$	538	539

TABLE IV (*continued*).

SLJ[a] State	Obs.[b] (cm^{-1})	Species[c]	Model[d] calc. (cm^{-1})	Fit[e] calc. (cm^{-1})
$^5D_2$	21 541	A_1	21 532	21 532
	565	$A_{2(1)}$	561	562
$^5D_3$	···	$B_{(2)}$		24 398
	···	$A_{(2)}$		415
	···	$B_{(2)}$		422
	···	$B_{(1)}$		429
	···	$B_{(1)}$		439
	···	$A_{(1)}$		445
	···	$A_{(2)}$		449
$^5L_6$	···	$A_{(2)}$		25 067
	···	$A_{(1)}$		095
	···	$B_{(1)}$		098
	···	$B_{(2)}$		144
	···	$A_{(1)}$		188
	···	$B_{(1)}$		238
	···	$A_{(2)}$		245
	···	$B_{(2)}$		256
	···	$A_{(1)}$		375
	···	$B_{(2)}$		390
	···	$B_{(1)}$		394
	···	$A_{(2)}$		408
	···	$A_{(1)}$		464

Gaps in the energy level structure at 25 464–35 000 cm^{-1}[f]

Energy range (cm^{-1})	Energy gap (cm^{-1})
25 465–26 158	693
28 826–30 910	2084
31 838–33 136[g]	1298

[a] The leading eigenvector component is shown.

[b] Values in cm^{-1} vacuo from Ref. 7. The level at 2894 cm^{-1} was not included in the parameter fitting process, and a reported level at 2847 cm^{-1} was excluded.

[c] Symmetry species from Ref. 7. In cases where the sub species A_1, A_2, B_1 or B_2 was not identified by experiment, or the calculated symmetry was different than that assigned in Ref. 7, the subscript is shown in parentheses.

[d] Computed level structure based on approximate free-ion parameters estimated for Eu^{3+} from apparent systematic trends together with the crystal-field parameters of Sm^{3+}:LaF_3.

[e] The energy level parameters used to compute these levels are given in Table I.

[f] In most of the energy range from 25 465–50 000 cm^{-1} the density of computed crystal-field components is high. Since the fit parameters are approximate, and no experimental results are available for this region, we have indicated the few gaps of at least 650 cm^{-1} where no levels are computed to occur in the 25 465–35 000 cm^{-1}.

[g] A single $J = 0$ level ($^3P_0$) is computed to occur in this range at 32 958 cm^{-1}.

or odd and whether J is even or odd. This table also gives the correct symmetry for $M = 0$ states by regarding these states as plus states for $|M|$ even.

Symmetry for the eigenvectors is shown in Table IV. In all cases the A or B nature of the symmetry species from the experimental assignments[7] and the calculation agrees. Since

TABLE V. Character table for each of the four symmetry species of the C_{2v} point group.

Species	C_{2z}	σ_{xz}	$\|M\|$	J even	J odd
A_1	1	1	even	plus	minus
A_2	1	−1	even	minus	plus
B_1	−1	1	odd	minus	plus
B_2	−1	−1	odd	plus	minus

the eigenvalue calculation is partitioned into one for $|M|$ even and another for $|M|$ odd, this part of the symmetry classification was simple to impose as a constraint on the fit of energy levels. For two levels in the $^7F_4$ state, the symmetry species A_1 and B_1 could not be distinguished experimentally.[7] Only one assignment consistent with the energy level scheme could be made in each case.

The calculated symmetry subscript, 1 or 2, is shown in parentheses in Table IV if it differs from the experimental assignment. Since the eigenvalue calculation was not partitioned into plus and minus states, and thus experimental information about symmetry subscripts was not introduced as a constraint on the fitting, it is not too surprising that half the calculated and experimental symmetry subscripts disagree. This disagreement should be viewed as reminder that our understanding of the electronic structure for rare earth ions in the LaF_3 lattice is not yet complete with respect to the details of the eigenfunctions of these energy levels.

Er^{3+}:LaF_3 ($4f^{11}$)

Analyses of the heavy lanthanides in LaF_3 were developed starting with the analysis of the spectrum of Er^{3+}:LaF_3 and working back toward Gd^{3+}. The normal light lanthanide ion model for Gd^{3+} would have been Eu^{3+}, but it is itself poorly established experimentally.

The absorption and fluorescence spectra of Er^{3+}:LaF_3 measured at 77 K, which included levels up to ~39 500 cm^{-1}, were reported by Krupke and Gruber.[47] A subsequent investigation[48] included measurements at ~4 K in the range 6000–50 000 cm^{-1}. We have made additional spectroscopic measurements at low temperature, so that the levels recorded in Appendix V[35] represent a composite of published results and in a number of cases a reevaluation[14] of results originally given in Ref. 48.

An important aspect in the analysis of the Er^{3+}:LaF_3 spectrum is the continuing string of isolated free-ion states extending up to ~28 000 cm^{-1} with major absorption features corresponding to each expected crystal-field component. The extent of the experimental data left little room for more than one interpretation. While there is excellent correlation between the observed and computed patterns of crystal-field splitting, there is some apparent inadequacy of the free-ion part of the model to fully reproduce centers of gravity of certain groups. The final parameter fitting included ~80% of the free-ion states in the whole configuration.

Fit values of some parameters turned out to be inconsistent in magnitude with those expected from apparent regularities across the series. However, the values of those pa-

rameters were surprisingly amenable to change when constraints were introduced. By holding γ and T^2 constant, the values of F^k were forced to assume magnitudes consistent with systematic values. Thus the final fit to the data shown in Table I is not that recorded in Ref. 14, but one in which the F^k are more consistent with series trends; however, the energy levels computed with the new parameters were essentially identical to those obtained earlier without the constraints on γ and T^2.

Tm^{3+}:LaF_3 ($4f^{12}$)

Most of the crystal-field components of the states of Tm^{3+}:LaF_3[49] have been experimentally identified,[13] and are given in Appendix VI.[35] Nevertheless, the number of assigned states is not sufficient to adequately determine all the parameters of the theoretical model. Crystal-field parameters determined for Er^{3+}:LaF_3, together with free-ion parameters for Tm^{3+} established earlier,[49] were used to compute a model set of energy levels.[13]

Transitions between the ground state and excited multiplet states in the $4f^{12}$ configuration of Tm^{3+} all occur in the range 5000–40 000 cm^{-1}, except for that to $^1S_0$. As in Pr^{3+}, the $^1I_6$ state in Tm^{3+} was predicted to have a large total splitting (about 500 cm^{-1}); however, in Tm^{3+} the group is isolated in energy from other free-ion groups, and some assignments could be made.

Yb^{3+}:LaF_3($4f^{13}$)

Classification and analysis of lines assigned to the fourth spectrum of atomic Yb, Yb IV, places the $^2F_{7/2}$–$^2F_{5/2}$ ground term interval at 10 214.0 cm^{-1}.[50] This yields a value of the spin–orbit coupling constant of 2918 cm^{-1}. Rast and coworkers[51] reported both the absorption and fluorescence spectra of Yb^{3+}:LaF_3, and interpreted their results as indicating levels of $^2F_{5/2}$ at 10 260, 10 430, and 10 660 cm^{-1}. Two excited levels belonging to the ground $^2F_{7/2}$ state were placed at 185 and 401 cm^{-1}, leaving one level unidentified. The electronic structure exhibited by Yb^{3+} in several different hosts has been summarized by Dieke,[1] with generally similar crystal-field splitting patterns to that reported for Yb^{3+}:LaF_3. The computed energy-level scheme, Table VI, using crystal-field parameters for Tm^{3+}:LaF_3, provided a useful basis for interpretation. The correlation of computed energies for the ground $^2F_{7/2}$ state with the two reported states suggests that a low energy state near 50 cm^{-1} has not been observed. The fact that both absorption to the fluorescence from a level near 10 260 cm^{-1} have been reported[51] indicates that this is undoubtedly the lowest energy crystal-field component of the $^2F_{5/2}$ excited state. We have confirmed the existence of strong sharp bands at 10 260 and 10 430 cm^{-1} by measuring the spectrum of 1% Yb^{3+}:LaF_3. However, no clear evidence was obtained for a band near 10 660 cm^{-1}. As pointed out by Rast *et al.*, there is a broad shoulder to the higher energy side of the 10 430 cm^{-1} band. The model calculation does place a level in the 10 450–10 750 cm^{-1} energy range. The value of ζ determined by a fit to the data was, within the error, the same as tht for Yb IV.

TABLE VI. Experimental and computed energy level structure for Yb^{3+}:LaF_3.

SLJ state	Obs.[a] (cm^{-1})	Calc.[b] (cm^{-1})	O − C
$^2F_{7/2}$	0	26	−26
	...	78	
	185	178	7
	401	382	19
$^2F_{5/2}$	10 260	10 301	−41
	430	389	41
	(660)[c]	571	

[a] Reference 51 (cm^{-1} vac).
[b] Parameter values are given in Table I.
[c] Not included in the parameter fitting.

Ho^{3+}:LaF_3 ($4f^{10}$)

An extensive investigation of the absorption and fluorescence spectra of Ho^{3+}:LaF_3 has been reported by Caspers, Rast, and Fry (CRF).[52] Our experiments marginally extended the number of states that could be assigned.[14] The experimental level energies shown in Appendix VII[35] are similar to those reported for Ho^{3+}:$LaCl_3$.[53]

The preliminary energy level calculation for the Ho^{3+}:LaF_3 system, with approximate free-ion parameters and crystal-field parameters derived for Er^{3+}:LaF_3, provided an excellent correlation with the measured spectra. Numerous levels were computed to be essentially degenerate in energy, thus predicting that the spectrum should appear somewhat less congested than might have been expected.

Interpretation of this absorption spectrum was complicated by the existence of a ground state crystal-field component at 4.5 cm^{-1}. This level appeared as a satellite on the majority of the bands we observed at 4 K. Most of our results correlated fully with the extensive data reported by CRF who did perform measurements at ~1.5 K, where the 4.5 cm^{-1} state was not significantly populated. In Appendix VII,[35] we only report levels from CRF corresponding to features found in our spectra,[14] or where there was some evidence that our observations might have been limited by resolution.

In the final analysis, 204 levels served to define the energy level parameters in the present case compared to 128 in Ho^{3+}:$LaCl_3$.[53] In Ho^{3+}:LaF_3 the preliminary and final crystal-field parameters, except for B_0^2, were similar and the model appears to be adequate. For reasons we could not discern, when allowed to vary freely, B_0^2 assumed a value of about half of that expected from trends in the series. Assignment of the value 240 cm^{-1} did not appear to perturb any of the other parameters, Table I. Similarly, series-inconsistent values of γ and T^2 were obtained when these parameters were free. In the analysis of the Ho^{3+}:$LaCl_3$ spectrum, some residual problems in the fit were attributed to the crystal-field part of the Hamiltonian. There are clear differences in the values for γ and in some of the T^k in the two crystals, but these parameters are not independent of the F^k which are also larger for Ho^{3+}:LaF_3.

Dy^{3+}:LaF_3 ($4f^9$)

Absorption and fluorescence spectra of Dy^{3+}:LaF_3 including levels up to $\sim 32\,000$ cm^{-1} have been reported.[11,15,54] The results included in Appendix VIII,[35] at $\geqslant 5800$ cm^{-1} represent for the most part observations made in the present investigation. The initial adjustment of atomic and crystal-field parameters was based on assignments made to isolated groups of levels; final parameters are given in Table I. Many of the assignments included all the expected crystal-field components of a particular state.

Tb^{3+}:LaF_3 ($4f^8$)

The absorption spectrum of Tb^{3+}:LaF_3 represents a particularly challenging case for energy level structure analysis, and there do not appear to be previously reported investigations by others. Most of the band structure we observed was in the 26 000–40 000 cm^{-1} range. At higher energies the transitions in our $\sim 1\%$ doped crystals were too weak to be observed in absorption. The energies of the crystal-field levels assigned in the present investigation[16] are included in Appendix IX.[35] Both the low intensity and high density of levels have been cited as problems in interpreting the spectrum of Tb^{3+}:$LaCl_3$ were "safe" crystal-field analysis[1] did not extend above $\sim 26\,000$ cm^{-1}.

Since only a fraction of the $4f^6$ configuration is found at $\leqslant 50\,000$ cm^{-1}, it is not surprising that the F^k parameters are not well established by the existing data. Constraints were adopted to yield a parameter set that did provide an excellent correlation between observed and computed level energies, Table I, and was also consistent with systematic trends in parameter values.

Gd^{3+}:LaF_3 ($4f^7$)

The energy levels of the ^6P and ^6I groups in Gd^{3+}:LaF_3 were reported both by Caspers *et al.*[55] and by Schwiesow and Crosswhite.[56] These experimental results were subsequently extended to include the ^6D and ^6G crystal-field states in the 40 000–50 000 cm^{-1} range.[57] The data recorded in Appendix X[35] are a composite of the results published in Refs. 56 and 57.

A crystal-field analysis of the spectrum of Gd^{3+}:LaF_3 to $\sim 37\,000$ cm^{-1} demonstrated that good agreement with experiment could be achieved by assuming a hexagonal site symmetry.[11,56] In a complete free-ion and crystal-field matrix element diagonalization in C_{2v} symmetry,[16] the obvious problem lies in having experimental results for such a small fraction of the whole configuration. This was also encountered in Tb^{3+}:LaF_3, but is even more evident in the present case.

Crystal-field parameters for Tb^{3+} combined with the free-ion parameters for Gd^{3+}:LaF_3,[57] provided the basis for a model calculation. In each free-ion group, deviations of the model-computed levels from observed band energies were less than 12 cm^{-1}, for assignments in the range 32 000–49 250 cm^{-1}.[16] In the parameter fitting, with additional experimental levels near 50 000 cm^{-1} included, only seven free-ion parameters were freely varied, Table I. The crystal-field parameters are those of Tb^{3+}:LaF_3.

Comparison of the crystal-field parameters for Eu^{3+}:LaF_3 with those for Tb^{3+}:LaF_3 reveal considerable differences, particularly in the sixth degree terms. However, when the crystal-field parameters of Eu^{3+}:LaF_3 were combined with the free-ion parameters of Gd^{3+}, the resulting fit to the observed crytal-field splitting in Gd^{3+}:LaF_3 was also satisfactory, giving $\sigma = 11$ cm^{-1}. Thus, we find that more than one set of C_{2v} crystal-field parameters yields satisfactory correlation with experiment. This type of ambiguity had already been revealed by the difference between our crystal-field parameter set for Gd^{3+}:LaF_3 in D_{3h} symmetry[11] and that of Schweisow and Crosswhite,[56] both quite adequately reproducing the available experimental data.

As a result of the special properties of the $4f^7$ configuration, first-order crystal-field matrix elements vanish and any explanation of observed splittings of the ground or excited states must involve at least second or higher order crystal-field interactions.[4,58] The ordering of the crystal-field components in the ground state is dependent on the sign of B_0^2, and is $\pm 7/2$, $\pm 5/2$, $\pm 3/2$, $\pm 1/2$ with $\pm 7/2$ calculated lowest for $+B_0^2$. A positive sign for B_0^2 appears to be consistent with EPR results for Gd^{3+} in LaF_3 [59] and in fluorozirconate glass,[60] and in agreement with the crystal-field analysis assuming D_{3h} site symmetry.[11]

In the treatment of the optical spectra of Ln^{3+}:LaF_3, assuming an approximate C_{2v} symmetry, we obtain a negative B_0^2 term. However, if instead of the approximate C_{2v} symmetry we were to use C_2 symmetry,[12] alternate sets of crystal-field parameters, one with $+B_0^2$, the other with $-B_0^2$, depending on whether the z axis is taken parallel or perpendicular to the crystal c axis, could be determined to give equally good representations of the actual data.

SYSTEMATIC TRENDS

In the work reported here, each lanthanide was initially treated independently with as many of the parameters of the model varied as could be well established from the available data base before any intercomparison along the series was attempted. In all cases, the subsequent imposition of constraints to preserve what appeared to be systematic trends in parameter values, could be made without any significant change in the goodness of fit to the experimental levels. Thus to a large extent the constraints were imposed on parameters that turned out to be relatively insensitive to the available experimental data base. The free-ion parameters in Ln^{3+}:LaF_3 were expected to approach those of the gaseous free-ion. In fact, for Pr^{3+}:LaF_3 the F^k values are 96%–97% of those for Pr IV, while the values of ζ for Ce^{3+}, Pr^{3+}, and Yb^{3+}:LaF_3 are, respectively, 93%, 98%, and 100% of the corresponding gaseous free-ion values.[25] It was found that extremely good fits to experimental data could be obtained with some parameters nearly constant over the series, but trends in other parameters were evident.

Atomic (free-ion) parametrization

It has been pointed out that comparison of values of F^k and ζ calculated using *ab initio* methods (which we designate as HFR)[25] with values of these integrals established by

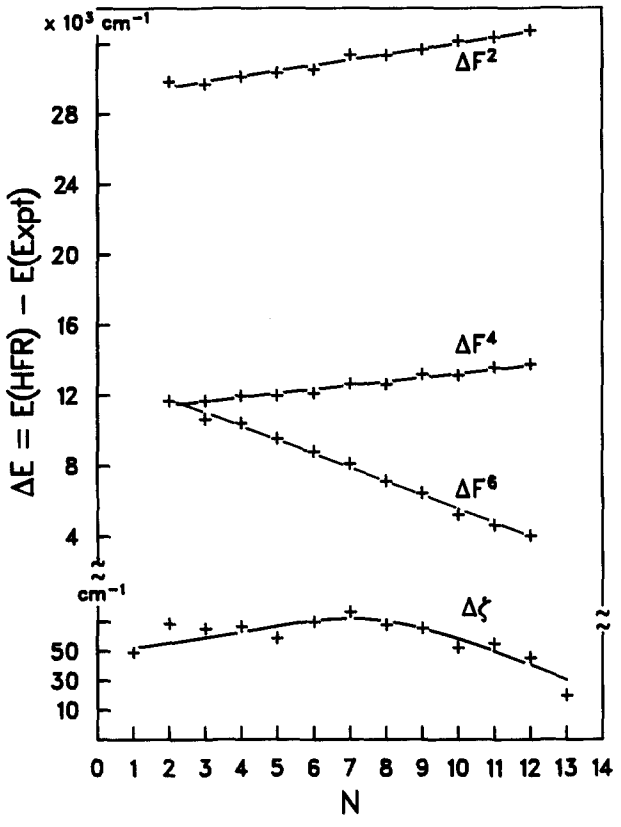

FIG. 1. Variation of the energy difference, $\Delta E = E(\text{HFR}) - E(\text{EXPT})$, between the HFR computed energy and that determined from experimental data as a function of number of f electrons.

fitting experimental data, results in energy differences, i.e., $E(\text{HFR}) - E(\text{EXPT}) = \Delta E$ which tend to show a constancy over the series that can be useful for purposes of extrapolation.[10,25] The differences between HFR and experimental F^k and ζ values for Ln^{3+}:LaF_3 are plotted in Fig. 1. While changes in ΔF^2 and ΔF^4 over the series turn out to be small enough to be treated as essentially constant over a limited range of N, this is a much less satisfactory assumption for ΔF^6. In addition, we find that the slope of ΔF^6 is opposite to that of ΔF^2 and ΔF^4. Errors in ΔF^k are within the width of the lines indicated in Fig. 1. When we reexamined the data for Ln^{3+}:$LaCl_3$,[10,11,25] we found perhaps less distinct but certainly similar evidence for a negative slope in ΔF^6. The greater magnitude of the slope for $k = 6$ compared to $k = 2$ or 4 places a severe limit on the range in which ΔF^6 values can be assumed to be constant.

Variation of $\Delta\zeta$ over the series was similar to that found for Ln^{3+}:$LaCl_3$[25] showing a maximum near $N = 7$. Individually, both the HFR and the experimental values of ζ plotted as a function of N are well represented by cubic equations. No constraints were placed on the parameter fitting. However, mismatch in the HFR and the fit results obviously reaches a maximum at $N = 7$, then decreases.

Some of the principal effects of configuration interaction were added to the Hamiltonian in the form of two- and three-body operators that operate wholly within the f^N configuration. The two-body electrostatic corrections α and β show relatively little variation over the series but appear to decrease with increasing N. For β in Ln^{3+}:LaF_3 the slope is opposite to that in Ln^{3+}:$LaCl_3$. A slow increase in γ as a function of N for Ln^{3+}:LaF_3 is now apparent, Fig. 2. Apparent systematic trends indicate that α for Pr^{3+}:LaF_3 should be > 16, and would argue against our suggested interpretation of the energies of the $^1I_6$ group components. The behavior of T^2 seems to parallel that of γ, but other T^i are essentially constant.

Different conventions have been suggested for introducing H_{ss} (spin–spin), H_{soo} (spin–other-orbit), and electrostatically correlated spin–orbit (EL–SO) interaction, into the analysis of f-electron systems. We adopted the use of the parameters M^0, M^2, and M^4, for H_{ss} and H_{soo}. Since there were significant shifts in the values of M^h dependent upon the values of P^f, it appears to be useful to vary both sets simultaneously. Pasternak and Goldschmidt have stressed the necessity for including all spin-dependent parameters in the analysis of $3d^N$ configurations.[61] A reasonable course of

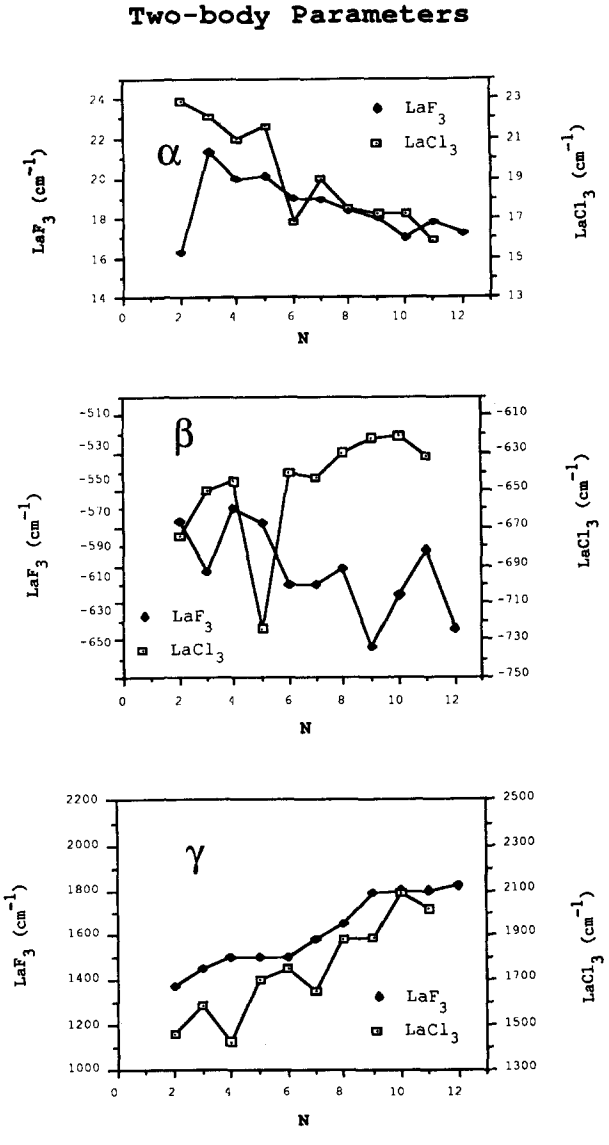

FIG. 2. Variation of the parameters α, β, and γ (cm^{-1}) for Ln^{3+}:LaF_3 and Ln^{3+}:$LaCl_3$ as a function of number of f electrons (N).

action for the M^h is to use ratios for M^2/M^0 ($=0.56$) and M^4/M^0 ($=0.38$) that result from Hartree–Fock calculations, allowing only M^0 to vary freely.

The situation with respect to limiting the number of P^f parameters freely varied is more complicated than for the M^h. While the parameter values determined by fitting to experimental data are consistent with those computed via *ab initio* methods,[62] no complete set of *ab initio* values is available. Since the mechanism of the EL-SO interaction involves a product of spin–orbit and electostatic matrix elements, ratios of the p^f identical to the ratios of the F^k have been used for the lanthanides $F^4/F^2 \sim 0.75$ and $F^4/F^2 \sim 0.5$.[25] However, when Judd and co-workers used experimental results for Pr IV ($4f^2$) as the basis for determining values of the P^f, they found that when freely varied, P^2 and P^4 were indeterminate, and P^6 assumed a large negative value.[29] It was speculated that P^6 might, in fact, be reproducing effects such as the expansion of the $4f$ eigenfunction as the energy is increased, suggesting that large negative contributions to P^6 could arise if interactions with the continuum were considered. In the present investigation, our results were consistent with those reported previously.[29] Additionally, we found that in a fit of data for Pr III ($4f^3$), Ref. 63, as was the case for Pr IV, the value of P^6 was well determined but negative.

Since the M^h and P^f values do interact, we chose a modified convention. The parameter P^2 was varied freely while P^4 and P^6 were constrained by the ratios $P^4/P^2 = 0.5$ and $P^6/P^2 = 0.1$. Thus, we have deemphasized P^6 with the knowledge that it can assume negative values when it is allowed to vary freely. Using the indicated constraints, only in the fit of Pr^{3+}, Table I, did P^2 assume a negative value. Over the series, the constraints adopted resulted in minor changes in the values of M^0, and a reasonably uniform increase in P^2 with increasing atomic number in the lighter half of the series but less overall change in the heavier lanthanides.

Crystal-field parametrization

While the practice of treating the effects of the crystalline field on a lanthanide ion by supplementing the free-ion Hamiltonian with a sum of single-electron operators has generally yielded a very good correlation with experimental results, some exceptions, such as the $^3K_8$ group of Ho^{3+}:$LaCl_3$, and the $^1D_2$ state of Pr^{3+}:$LaCl_3$, have been recognized, and methods of improving the model have been explored.[64–67]

The effect of the crystalline environment is to reduce the magnitude of the free-ion parameters, but in the case of $4f^2$ we see that this reduction is relatively small as we compare values of F^k and ζ for Pr IV[25] and Pr^{3+}:LaF_3. Some of the difficulties that arose in fitting crystal-field levels in Ln^{3+}:$LaCl_3$ (D_{3h} symmetry) were not apparent in fitting the corresponding groups in the LaF_3 host. However, one must recognize that for LaF_3 we deal with a nine parameter crystal-field model compared to four parameters for D_{3h} symmetry, and thus there is more flexibility in the lower symmetry parametrization. Since Zeeman or polarization data are not normally useful in identifying crystal-field components in the fluorides, in making assignments for the best agreement with the calculated energies, some discrepancies may have been hidden. Thus, we cannot conclude on the basis of the fits to experimental data that the single-electron crystal-field model works better for the fluorides than the chlorides.

One of the critical aspects of crystal-field parametrization is the choice of initializing values. We have relied on lattice sum results of Morrison and Leavitt.[2,12] The superposition model of Newman[68,69] offers an alternative method for calculation of starting crystal-field parameters based on a knowledge of the crystal structure. It can also be used to reduce the number of parameters freely varied by providing values for the ratios of selected parameters. However, both the lattice sum calculations[12] and the superposition model require detailed crystallographic data. The approach we have used yields sets of parameters that are of the same magnitude and sign as the real parts of the corresponding C_2 symmetry parameter sets, but it is based on an approximation of the actual crystal structure.

Trends in the magnitudes of the crystal-field parameters for Ln^{3+}:LaF_3 as a function of the number of f electrons are shown in Figs. 3–5. One would expect to decrease in magni-

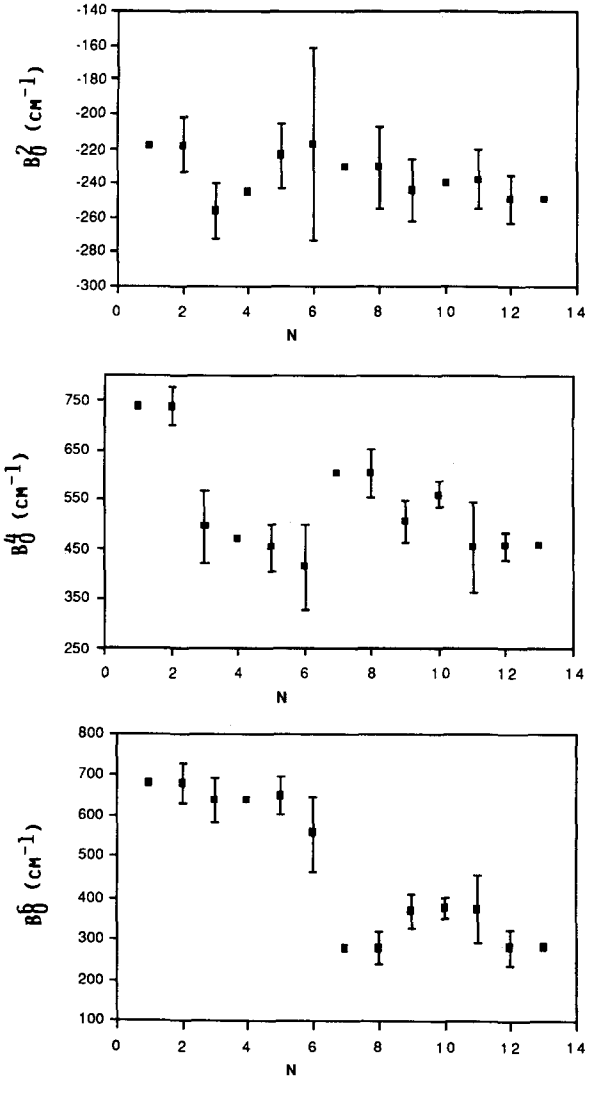

FIG. 3. Variation of the crystal-field parameters B_0^2,B_0^4, and B_0^6 (in cm^{-1}) for Ln^{3+}:LaF_3 as a function of number of f electrons (N).

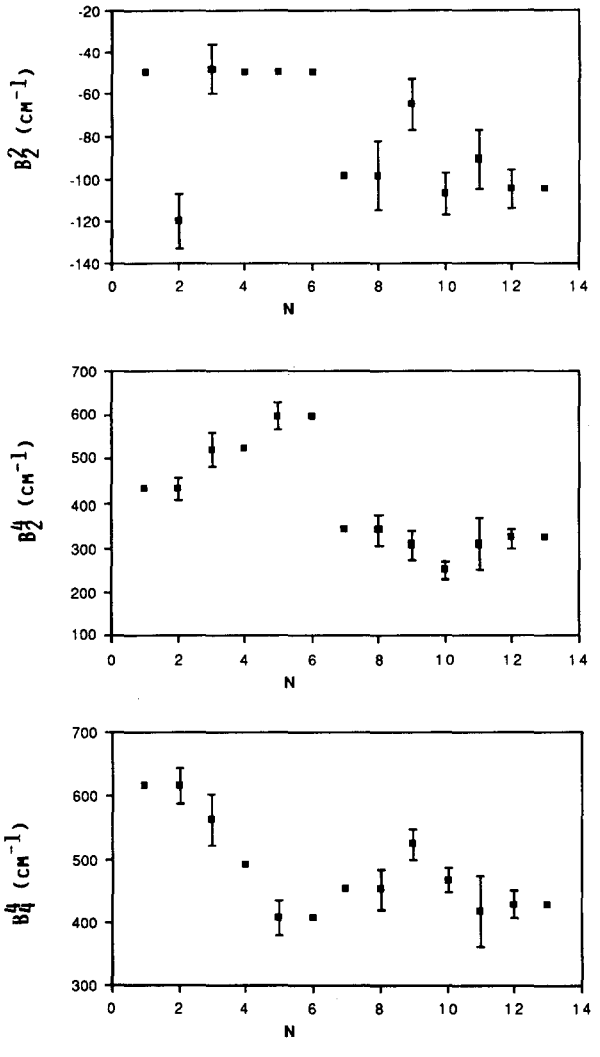

FIG. 4. Variation of the crystal-field parameters B_2^2,B_2^4, and B_4^4 (in cm^{-1}) for Ln^{3+}:LaF_3 as a function of number of f electrons (N). Error bars are indicated.

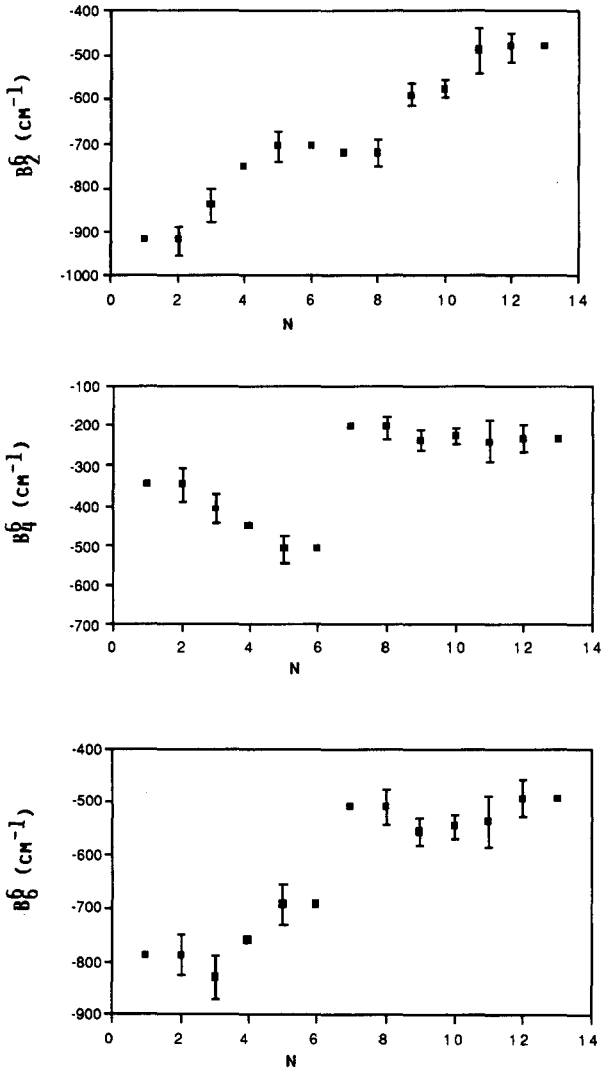

FIG. 5. Variation of the crystal-field parameters B_2^6,B_4^6, and B_6^6 (in cm^{-1}) for Ln^{3+}:LaF_3 as a function of number of f electrons (N).

tude of these parameters over the series due to the increased nuclear charge that the electrons experience. As the electron orbits are pulled in closer to the nucleus, the effect of the crystal field should be reduced even though the network of F^- ions may to a certain extent collapse around the impurity ion as its radius decreases. The change should be greatest early in the series where ionic radii are exhibiting their greatest relative decrease. However, not all the parameters follow the expected trends.

As shown in Fig. 3, B_0^2 appears to be essentially constant over the series, matching the expectation of Morrison and Leavitt.[12] B_2^2 was not well defined in a number of fits, and thus was frequently not varied. All of the other parameters with the possible exception of B_2^6 are best represented by different lines for the light and heavy ends of the series. All except B_0^4 and B_2^6 are essentially constant over the second half of the series.

For many of the parameters there is a marked discontinuity in magnitude between Eu^{3+} and Tb^{3+}; however, we found that the crystal-field parameters for both Eu^{3+} and Tb^{3+}:LaF_3 very adequately described the limited data for Gd^{3+}. For B_0^4 and possibly B_4^4 and B_4^6, there is an increase in the magnitude of the parameters for Tb^{3+} compared to Eu^{3+}, but for all others there is a decrease. For comparison, parameters[10] for Ln^{3+}:$LaCl_3$ are plotted in Fig. 6. Only the $k = 6$ terms show the discontinuity and the decrease in magnitude at the center of the series. Richardson and co-workers have carried out a related analysis of the spectra of Ln^{3+} in cubic $Cs_2NaLnCl_6$.[70] Their parameter values also exhibit a marked decrease across the center of the series for $k = 6$. The scatter is large for $k = 4$ so that the existence of a break is not clear. Thus, the common features already cited do not appear to be restricted to a particular symmetry or type of ligand.

Judd has interpreted the drop in the sixth-rank parameters in going from Eu^{3+} to Tb^{3+}:$LaCl_3$ as an indication of the need to include two-electron operators in the crystal-field Hamiltonian.[65] One-electron operators, U^k, change sign at the center of the series but the likely two-electron operators would not. Thus if contributions from two-elec-

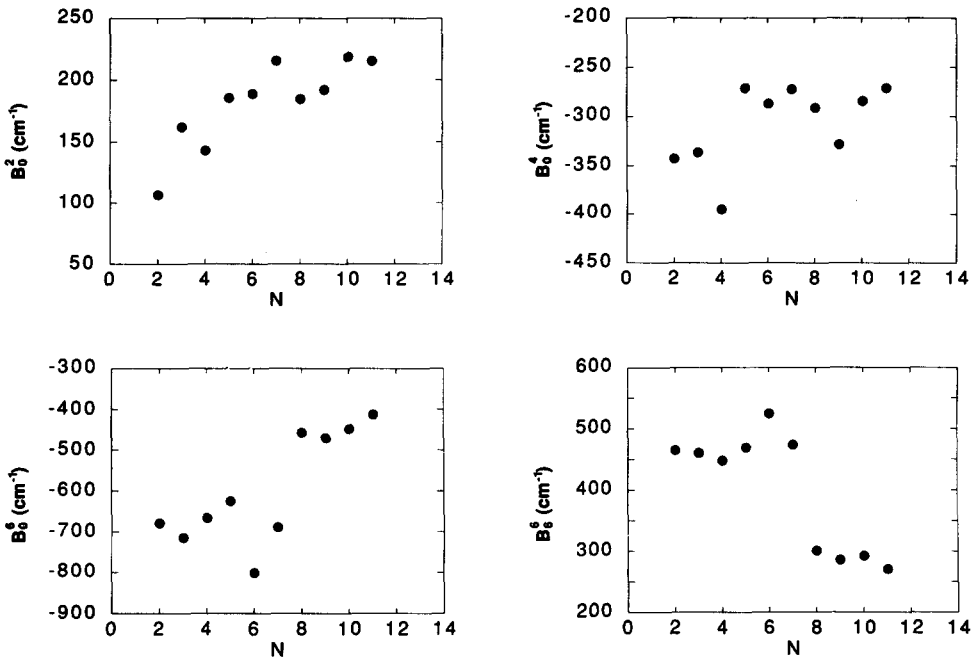

FIG. 6. Variation of the crystal-field parameters B_0^2, B_0^4, B_0^6, and B_6^6 (in cm^{-1}) for Ln^{3+}:$LaCl_3$ as a function of number of f electrons (N).

tron operators are being absorbed by the crystal-field parameters, there would be a break when crossing the center of the series. If the two-electron terms were properly parametrized and not included in the one-electron crystal-field parameters, the latter would presumably vary smoothly across the series.

There are a number of possible two-electron operators which could be added to the crystal-field Hamiltonian,[71] but a large part of the effect may be parametrized as a spin-correlated crystal-field (SCCF), which requires only three additional parameters.[64,67] The one-electron crystal-field operator is supplemented by

$$H_{\mathrm{SCCF}} = \sum_{k,q,i} b_q^k s_i \cdot SC_q^{(k)}$$

and the ratio $c_k = b_q^k / B_q^{(k)}$ is used as a measure of the importance of the two-electron crystal-field. This has the advantage of being independent of the normalization used to define the crystal-field parameters. Values of c_k have been obtained for Gd^{3+} and Ho^{3+} in $LaCl_3$,[72] for three lanthanide ions in Cs_2NaYCl_6,[73] and for Nd^{3+} in fluoride matrices.[74] However, the improvement in the fit in these investigations was not enough to clearly establish the importance of this particular mechanism. In a recent paper, the role of orthogonal operators in representing the correlation crystal-field was examined.[75] Again, Gd^{3+} and Ho^{3+}:$LaCl_3$ data were chosen, but consistent results were limited to parameters related to the sixth rank SCCF. These results are of the correct sign to remove the drop in the center of the series. A positive c_k has been shown to result from a covalency (charge transfer) mechanism.[67]

One of the important applications of a systematic set of lanthanide energy level parameters is found in the calculation of intensity correlations using the Judd–Ofelt theory.[76,77] The matrix elements of the transition probability in absorption and luminescence are most appropriately computed from a systematic set of atomic parameters. The intensity parameters can then be determined semiempirically for any particular system from the observed variation in band intensities. We have already tabulated the matrix elements of $U^{(k)}$ based on an earlier more approximate assessment of the atomic parameters.[11] While the present results show deficiencies in some of the parameter trends originally deduced, the discrepancies are not sufficiently serious to warrant recalculation of the matrix elements.

The widely circulated Dieke chart of energy level structure in the lanthanides[1] was limited by the extent of available analyses of the spectra of Ln^{3+}:$LaCl_3$. In the present case, the observed spectra in LaF_3 form the basis for a consistent interpretive model for all trivalent lanthanides except Pm^{3+} and Eu^{3+} where we have extrapolated or interpolated to compute levels. Finally, we have prepared a new chart, Fig. 7, which is a complete representation for the energy range shown, based entirely on the computed energy level schemes of Ln^{3+}:LaF_3. In some cases, these energy levels are dominated by contributions from a particular Russell–Saunders term ^{2S+1}L, or at least by states with a particular value of J, the total angular momentum. We have labeled appropriately those levels where this type of parentage is clear. In many cases, however, the crystal-field split components are so dense and intermingled as to produce, on the scale of this figure, only a broad, solid band of levels with no single characteristic J value. For the higher energies, those greater than about 30 000 cm^{-1}, these dense bands of levels are common and our emphasis then is on indicating the few isolated regions in which a band gap of at least 400 to 500 cm^{-1} is suggested by our calculations.

CONCLUSIONS

Using a C_{2v} crystal field to approximate the C_2 site symmetry, we have been able to correlate extensive spectroscopic data for Ln^{3+}:LaF_3 with a consistent set of free-ion and

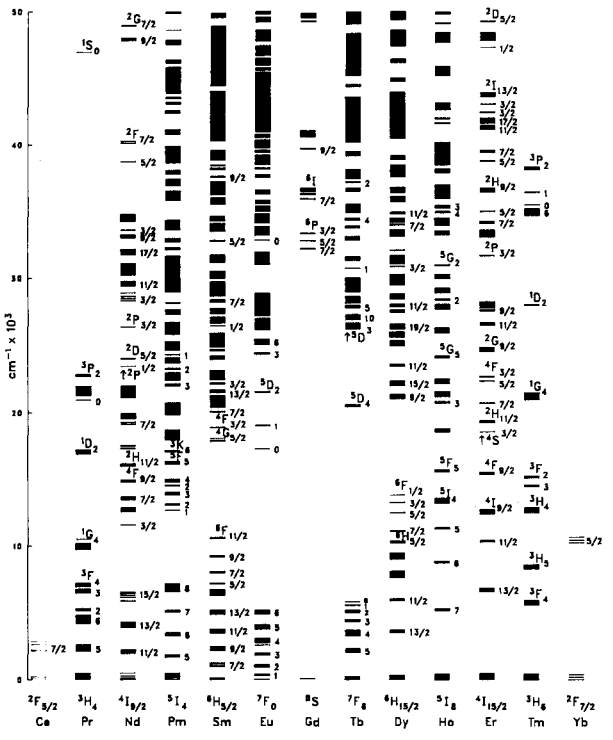

FIG. 7. Energy level structure of Ln^{3+}:LaF_3 based on computed crystal-field energies in the range 0–50 000 cm^{-1} with labels of ^{2S+1}L and/or J, where the dominant character of the levels can be clearly assigned.

crystal-field parameters. The rms deviations are all ~ 10–15 cm^{-1}. These results provide the basis for the most complete analysis of rare earth ions that is available in any host. We have drawn a number of conclusions regarding systematic trends in parameter values which should prove useful in analyses of other rare earth and actinide spectra, and which point out directions where further work is needed. Considering the inherent difficulty we experienced in defining the values of the free-ion parameters near the center of the series, it is evident that reservation must be exercised in evaluating published sets of atomic parameters derived by fits to severely limited data bases and without regard for systematics.

(1) The variations of F^k across the series are well represented by linear equations while those of ζ are much better represented by a cubic equation.

(2) The difference between HFR and empirical values for F^2 and F^4 (ΔF^2 and ΔF^4) increases slightly across the series while ΔF^6 decreases markedly. This is contrary to previous conclusions based on less complete data.

(3) The P^f parameters do not appear to have the same ratios as the F^k parameters, and we have obtained additional evidence for P^6 assuming negative values in some cases. This requires further investigation because the mechanism associated with the introduction of the P^f does not lead to negative values.

(4) Changes in magnitude of the crystal-field parameters across the series are in accord with previous indications of the importance of two-electron operators in the crystal-field Hamiltonian. There is some indication of the need for such terms with ranks 4 and 6. The magnitudes of B_0^4 and B_4^4 increase at the center of the series, whereas most other rank 4 and 6 parameters decrease. Thus, the variation of the crystal-field parameters is such that extrapolation from one half of the series to the other could lead to very erroneous estimates of parameter values.

While the model used contains a large number of parameters, very few of them change significantly over the series. Nevertheless, it is the inclusion of effective operators representing important classes of configuration interaction that has removed much of distortion, particularly of the F^k parameters, found in early analyses. The two- and three-body effective operator parameters tabulated here can be used directly in the initial efforts to analyze spectra of lanthanides in other matrices.

ACKNOWLEDGMENTS

The contribution of Hannah Crosswhite in developing the computer programs is gratefully acknowledged. Many others, students and visiting scientists, have made important contributions to this work as it progressed over a number of years.

[1] G. H. Dieke, in *Spectra and Energy Levels of Rare Earth Ions in Crystals*, edited by H. M. Crosswhite and H. Crosswhite (Wiley, New York, 1968).
[2] C. A. Morrison and R. P. Leavitt, in *Handbook of the Physics and Chemistry of Rare Earths*, edited by K. A. Gschneidner and L. Eyring (North-Holland, New York, 1982), Vol. 5, p. 461.
[3] B. R Judd, *Operator Techniques in Atomic Spectroscopy* (McGraw-Hill, New York, 1963).
[4] B. G. Wybourne, *Spectroscopic Properties of Rare Earths* (Wiley, New York, 1965).
[5] S. Hüfner, *Optical Spectra of Transparent Rare Earth Compounds* (Academic, New York, 1978).
[6] E. Y. Wong, O. M. Stafsudd, and D. R. Johnston, Phys. Rev. **131**, 990 (1963).
[7] U. V. Kumar, D. R. Rao, and P. Venkateswarlu, J. Chem. Phys. **66**, 2019 (1977).
[8] A. Zalkin, D. H. Templeton, and T. E. Hopkins, Inorg. Chem. **5**, 1466 (1966).
[9] D. E. Onopko, Opt. Spectrosc. (U. S. S. R.) **24**, 301 (1968); Opt. Spectrosc. (U. S. S. R.), Suppl. **4**, 11 (1968).
[10] H. M. Crosswhite, Colloq. Int. CNRS **255**, 65 (1977).
[11] W. T. Carnall, H. M. Crosswhite, and H. Crosswhite, Special Rep. 1977, Chemistry Division, Argonne National Laboratory, Argonne, IL.
[12] C. A. Morrison and R. P. Leavitt, J. Chem. Phys. **71**, 2366 (1979).
[13] W. T. Carnall and H. Crosswhite, J. Less-Common Metals **93**, 127 (1983).
[14] W. T. Carnall, G. L. Goodman, R. S. Rana, P. Vandevelde, L. Fluyt, and C. Görller-Walrand, J. Less-Common Metals **116**, 17 (1986).
[15] G. L. Goodman, W. T. Carnall, R. S. Rana, P. Vandevelde, L. Fluyt, and C. Görller-Walrand, J. Less-Common Metals **126**, 283 (1986).
[16] W. T. Carnall, G. L. Goodman, G. M. Jursich, R. S. Rana, P. Vandevelde, L. Fluyt, and C. Görller-Walrand, Inorg. Chim. Acta **139**, 275 (1987).
[17] Optovac Inc., North Brookfield, MA., 01535.
[18] M. J. Weber, in *Optical Properties of Ions in Crystals*, edited by H. M. Crosswhite and H. W. Moos (Wiley Interscience, New York, 1967), p. 467.
[19] I. Oftedahl, Z. Phys. Chem. **6**, 272 (1929); **13**, 190 (1931).
[20] K. Schlyter, Ark. Kemi **5**, 73 (1953).
[21] M. Mansmann, Z. Anorg. Allg. Chem. **331**, 98 (1964); Z. Krist. **122**, 375 (1965).
[22] R. P. Lowndes, J. F. Parrish, and C. H. Perry, Phys. Rev. **182**, 913 (1969).

[23]A. K. Cheetham, B. E. F. Fender, H. Fuess, and A. F. Wright, Acta Crystallogr. Sect. B **32**, 94 (1976).
[24]A. Zalkin and D. H. Templeton, J. Am. Chem. Soc. **75**, 2453 (1953).
[25]H. M. Crosswhite and H. Crosswhite, J. Opt. Soc. Am. B **1**, 246 (1984).
[26]K. Rajnak and B. G. Wybourne, Phys. Rev. **132**, 280 (1965).
[27]B. R. Judd, Phys. Rev. **141**, 4 (1966).
[28]H. Crosswhite, H. M. Crosswhite, and B. R. Judd, Phys. Rev. **174**, 89 (1968).
[29]B. R. Judd, H. M. Crosswhite, and H. Crosswhite, Phys. Rev. **169**, 130 (1968).
[30]H. H. Marvin, Phys. Rev. **71**, 102 (1947).
[31]P. Caro, J. Derouet, L. Beaury, G. Teste de Sagey, J. P. Chaminade, J. Aride, and M. Pouchard, J. Chem. Phys. **74**, 2698 (1981).
[32]H. H. Caspers, H. E. Rast, and R. A. Buchanan, J. Chem. Phys. **42**, 3214 (1965).
[33]U. V. Kumar, H. Jagannath, D. R. Rao, and P. Venkateswarlu, Ind. J. Phys. **50**, 90 (1976).
[34]Y. K. Voron'ko, V. V. Osiko, N. V. Savost'yanova, V. S. Fedorov, and I. A. Shcherbakov, Sov. Phys. Solid State **14**, 2294 (1973).
[35]See AIP document no. PAPS JCPSA-90-3443-63 for 63 pages of tables containing experimental and computed energy level structures for Ln^{3+}:LaF_3 where $Ln^{3+} = Pr^{3+}$, Nd^{3+}, Pm^{3+}, Sm^{3+}, Gd^{3+}, Tb^{3+}, Dy^{3+}, Ho^{3+}, Er^{3+}, and Tm^{3+}. Order by PAPS number and journal reference from American Institute of Physics, Physics Auxiliary Publication Service, 335 East 45th Street, New York, NY 10017. The price is $1.50 for each microfiche (98 pages) or $5.00 for photocopies of up to 30 pages, and $0.15 for each additional page over 30 pages. Airmail additional. Make checks payable to the American Institute of Physics.
[36]W. T. Carnall, P. R. Fields, and R. Sarup, J. Chem. Phys. **51**, 2587 (1969).
[37]E. Y. Wong, O. M. Stafsudd, and D. R. Johnston, J. Chem. Phys. **39**, 786 (1963).
[38]W. M. Yen, W. C. Scott, and A. L. Schawlow, Phys. Rev. **136**, A271 (1964).
[39]H. H. Caspers, H. E. Rast, and R. A. Buchanan, J. Chem. Phys. **43**, 2124 (1965).
[40]L. R. Elias, W. S. Heaps, and W. M. Yen, Phys. Rev. B **8**, 4989 (1973).
[41]C. D. Cordero-Montalvo and N. Bloembergen, Phys. Rev. B **30**, 438 (1984); **31**, 613 (E) (1985).
[42]C. G. Levy, T. J. Glynn, and W. M. Yen, J. Lumin. **31/32**, 245 (1984).
[43]R. A. Buchanan, H. E. Rast, and H. H. Caspers, J. Chem. Phys. **44**, 4063 (1966).
[44]H. Gerlinger and G. Schaak, Phys. Rev. B **33**, 7438 (1986).
[45]W. T. Carnall, H. Crosswhite, H. M. Crosswhite, and J. G. Conway, J. Chem. Phys. **64**, 3582 (1976).
[46]H. E. Rast, J. L. Fry, and H. H. Caspers, J. Chem. Phys. **46**, 1460 (1967).
[47]W. F. Krupke and J. B. Gruber, J. Chem. Phys. **39**, 1024 (1963); **41**, 1225 (1964); **42**, 1134 (1965).
[48]W. T. Carnall, P. R. Fields, and R. Sarup, J. Chem. Phys. **57**, 43 (1972).
[49]W. T. Carnall, P. R. Fields, J. Morrison, and R. Sarup, J. Chem. Phys. **52**, 4054 (1970).
[50]J. Sugar, V. Kaufman, and N. Spector, J. Res. Natl. Bur. Stand. **83**, 233 (1978).
[51]H. E. Rast, H. H. Caspers, and S. A. Miller, J. Chem. Phys. **47**, 3874 (1967).
[52]H. H. Caspers, H. E. Rast, and J. L. Fry, J. Chem. Phys. **53**, 3208 (1970).
[53]H. M. Crosswhite, H. Crosswhite, N. Edelstein, and K. Rajnak, J. Chem. Phys. **67**, 3002 (1977).
[54]J. L. Fry, H. H. Caspers, H. E. Rast, and S. A. Miller, J. Chem. Phys. **48**, 2342 (1968).
[55]H. H. Caspers, S. A. Miller, H. E. Rast, and J. L. Fry, Phys. Rev. **180**, 329 (1969).
[56]R. L. Schwiesow and H. M. Crosswhite, J. Opt. Soc. Am. **59**, 602 (1969).
[57]W. T. Carnall, P. R. Fields, and R. Sarup, J. Chem. Phys. **54**, 1476 (1971).
[58]B. G. Wybourne, Phys. Rev. **148**, 317 (1966).
[59]V. K. Sharma, J. Chem. Phys. **54**, 496 (1971).
[60]D. Furniss, E. A. Harris, and D. B. Hollis, J. Phys. C **20**, L147 (1987).
[61]A. Pasternak and Z. B. Goldschmidt, Phys. Rev. A **6**, 55 (1972).
[62]G. M. Copland, D. J. Newman, and C. D. Taylor, J. Phys. B **4**, 1388 (1971).
[63]J. Sugar, J. Opt. Soc. Am. **53**, 831 (1963).
[64]B. R. Judd, Phys. Rev. Lett. **39**, 242 (1977).
[65]B. R. Judd, J. Luminesc. **18/19**, 604 (1979).
[66]B. R. Judd, J. Phys. C **13**, 2695 (1980).
[67]D. J. Newman, G. G. Siu, and W. Y. P. Fung, J. Phys. C **15**, 3113 (1982).
[68]D. J. Newman, Adv. Phys. **20**, 197 (1971).
[69]Y. Y. Yeung and D. J. Newman, J. Chem. Phys. **82**, 3747 (1985).
[70]F. S. Richardson, M. F. Reid, J. J. Dallara, and R. D. Smith, J. Chem. Phys. **83**, 3813 (1985).
[71]S. S. Bishton and D. J. Newman, J. Phys. C **3**, 1753 (1970).
[72]H. Crosswhite and D. J. Newman, J. Chem. Phys. **81**, 4959 (1984).
[73]M. F. Reid and F. S. Richardson, J. Chem. Phys. **83**, 3831 (1985).
[74]C. K. Jayasankar, F. S. Richardson, M. F. Reid, P. Porcher, and P. Caro, Inorg. Chim. Acta **139**, 287 (1987).
[75]M. F. Reid, J. Chem. Phys. **87**, 2875 (1987).
[76]B. R. Judd, Phys. Rev. **127**, 750 (1962).
[77]G. S. Ofelt, J. Chem. Phys. **37**, 511 (1962).